JOURNAL OF MATERIALS SCIENCE 27 (1992) 5745–5750

Surface topographical variation of single-crystalline diamond grown in CO–H_2 plasma

TADASHI NAKAMURA, HIDEAKI ITOH, HIROYASU IWAHARA
Synthetic Crystal Research Laboratory, School of Engineering, Nagoya University, Furo-cho, Chikusa-ku, Nagoya 464-01, Japan

Microtopographical variations of {1 1 1} and {1 0 0} crystal surfaces of single-crystalline diamond grown by microwave-plasma chemical vapour deposition of the CO–H_2 reactant system were examined using scanning electron microscopy. A layer-by-layer epitaxial growth process was observed on both crystal surfaces. A number of epitaxial two-dimensional nuclei were formed at random on {1 1 1} surfaces, where small triangular growth layers spread with the same orientations as the outline of the original {1 1 1} basal plane. These spreading layers were found to leave an inverse triangular pit (so-called trigon) pattern as they joined each other. On the other hand, square growth layers spread in parallel directions to {1 0 0} basal plane, and they stacked in the ⟨1 0 0⟩ directions to form a pyramidal growth hillock.

1. Introduction

Many reports have been published on morphological observations of diamond single crystals prepared by chemical vapour deposition (CVD) on diamond seed crystals [1–6] or other substrate materials [1, 7–11]. However, few reports have been written on the surface microtopographs and their variation with CVD treatment time. This information is very important in order to investigate morphological control of vapour-grown diamond single crystals and to elucidate the growth mechanism.

The crystal sizes of spontaneously nucleated diamonds are so small in general that it is difficult to observe their surface microtopographs by conventional scanning electron microscopy (SEM). Using high-resolution SEM, Hirabayashi *et al.* [12–14] observed a detailed microstructure on {1 1 1} surfaces of diamond crystals which were synthesized by the hot-filament CVD method. They observed triangular tiles and triangular pits on {1 1 1} surfaces and suggested a layer-by-layer crystal growth mechanism of {1 1 1} surfaces. However, they did not observe the growth process by a direct method as a function of CVD treatment time.

On the other hand, cubo-octahedral diamond single crystals can be obtained by treating natural coarse diamond grains in a long-term run of CVD [15]. The grain sizes of grown diamond single crystals are about 300 μm in diameter, so that the microtopographical variation of the same place on one single crystal surface can be easily observed by conventional SEM as a function of treatment time. In the present work, the growth process of {1 1 1} and {1 0 0} surfaces of vapour-grown diamond single crystals is observed in detail by SEM and the growth mechanism is discussed.

2. Experimental procedure

The microwave plasma CVD apparatus and major experimental procedure were the same as those described in previous papers [15, 16]. Natural coarse diamond crystal grains (particle size about 200 μm) were used as seed crystals, which were placed on (1 0 0) silicon wafers for the growth experiments. The optimum conditions for growth of single crystalline diamond [15] were kept constant as follows; microwave power 550 W, total pressure 45 torr, total flow rate 200 ml min^{-1} and CO concentration 5 vol %. The crystals grown under these conditions were confirmed to be a single phase of diamond by both X-ray diffraction and micro-Raman spectroscopy [15]. Surface microtopographs were observed by SEM.

The seed crystals were first grown for 20 h, when rather smooth crystal surfaces of {1 1 1} and {1 0 0} were formed [15]. Then scanning electron micrographs of the same place of each {1 1 1} and {1 0 0} surface were taken at a CVD reaction time interval of 2 h and the specimen was replaced after photographing as it had been in the reactor. No surface coating of the as-grown crystals was carried out for electrical conduction.

3. Results and discussion

3.1. Topographical variation of {1 1 1} crystal surface

Fig. 1 shows the surface topographical variation of the same place on the (1 1 1) crystal surface with CVD treatment time. A traced pattern of the surface topography corresponding to the treatment time of 20 h (Fig. 1a) and 30 h (Fig. 1f) is illustrated in Fig. 2, where the lateral faces of large growth layers are dotted. The

0022–2461

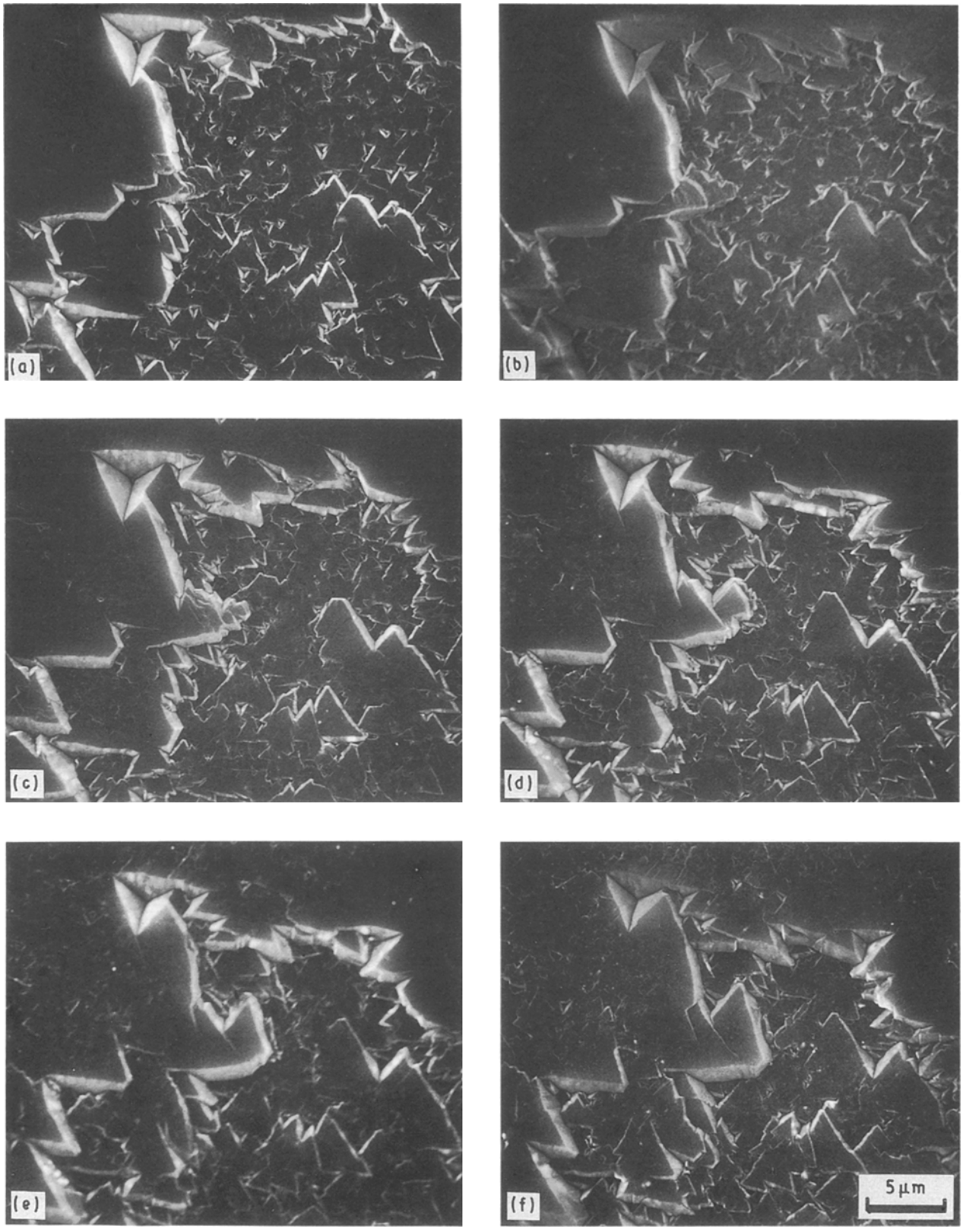

Figure 1 Topographical variation on (1 1 1) plane of diamond single crystal with treatment time: (a) 20 h, (b) 22 h, (c) 24 h, (d) 26 h, (e) 28 h, (f) 30 h.

(1 1 1) surface pattern is composed of triangular growth layers with various heights of about a few micrometres whose orientations are the same as the outline of the (1 1 1) basal plane [15]. Apparently these epitaxially growing layers extend in every direction parallel to (1 1 1) surface with elapse of CVD reaction time. The lateral facets of each growth layer are assigned as {1 0 0} or {1 1 1} planes. A model sketch of a triangular growth layer with indexed planes is shown in Fig. 3.

It is noted that the growth layers have a tendency to spread rapidly in directions so as to complete triangles. In other words, the growth rates of layers in $[\bar{2}\,1\,1]$, $[1\,\bar{2}\,1]$ and $[1\,1\,\bar{2}]$ directions are much higher than those in $[2\,\bar{1}\,\bar{1}]$, $[\bar{1}\,2\,\bar{1}]$ and $[\bar{1}\,\bar{1}\,2]$ directions. Fig. 4 shows the variation of the spreading length of a

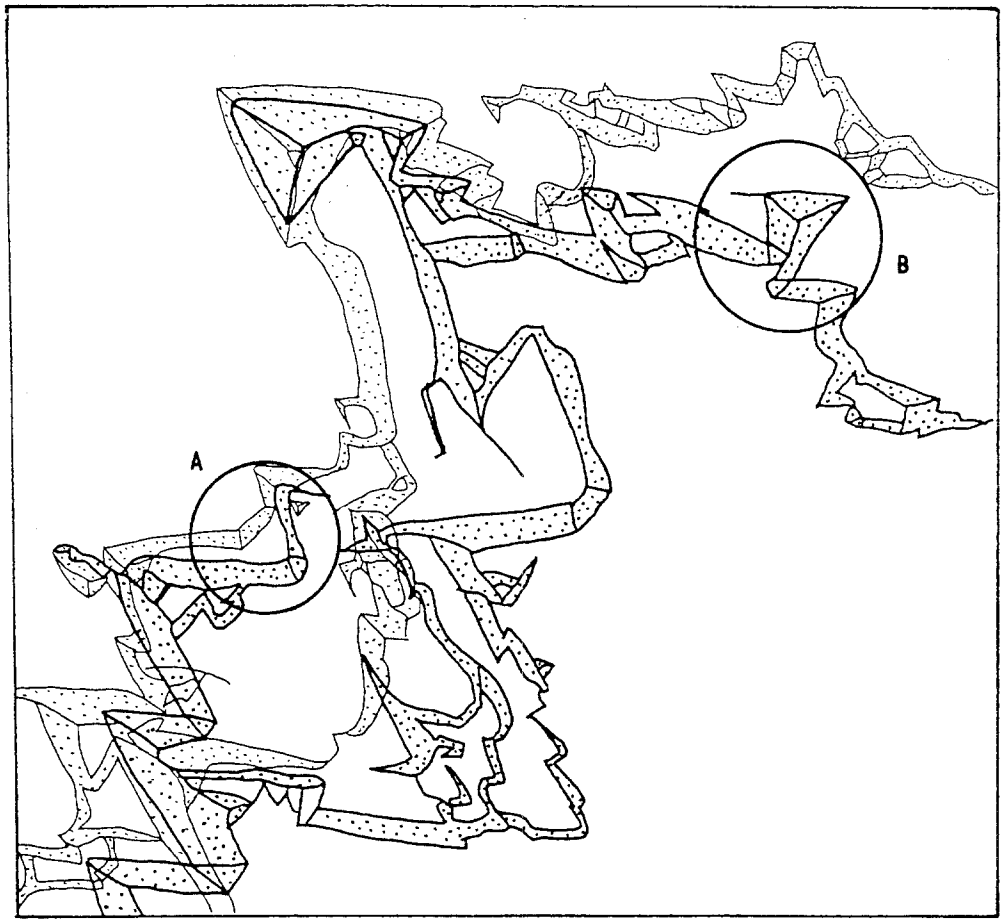

Figure 2 Traced pattern of surface topography in Fig. 1a (thin line; treatment time. 20 h) and Fig. 1f (thick line; treatment time 30 h).

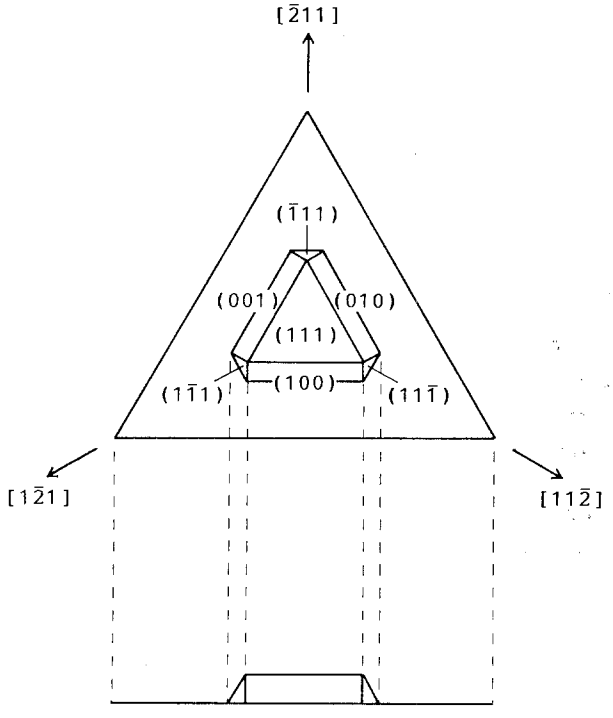

Figure 3 Sketch of a triangular growth layer with indexed planes on the (1 1 1) plane.

growth layer in two different directions of [1 1 $\bar{2}$] and [2 $\bar{1}$ $\bar{1}$], which were measured in the region A in Fig. 2 as a function of treatment time. It is confirmed that the faster growth rate of lateral {1 1 1} facets of the growth layer resulted in the formation of triangles. This mechanism of layer growth is illustrated in Fig. 5.

When triangular spreading layers with {1 0 0} lateral facets intersect, an inverse triangular pit is formed. The formation process of such triangular pits, whose orientations are reversed relative to the outline of the (1 1 1) basal plane [15], can be observed in Fig. 1 (typically in the region B in Fig. 2). These pits are analogous to the so-called "trigons" which have been observed in high-pressure synthesis of diamond [17]. A schematic model for the formation of a trigon is

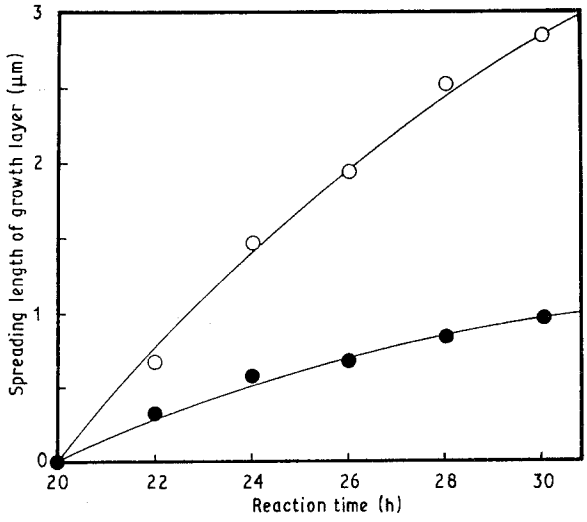

Figure 4 Spreading length of a growth layer on (1 1 1) plane as a function of treatment time: (○) in [1 1 $\bar{2}$] direction, (●) in [2 $\bar{1}$ $\bar{1}$] direction.

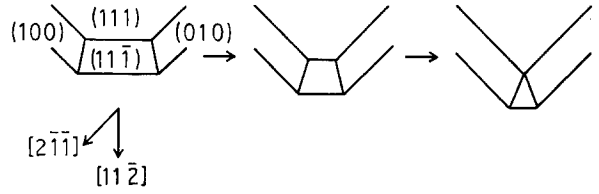

Figure 5 Topographical variation of spreading growth layer on (1 1 1) plane.

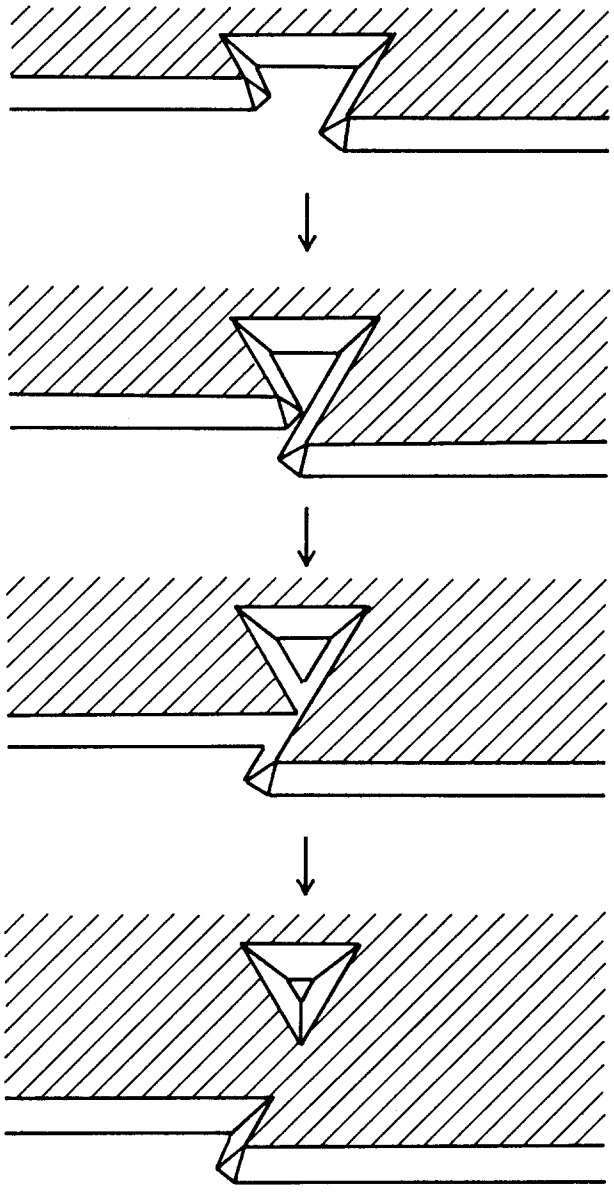

Figure 6 Formation model of a trigon on {1 1 1} surface.

shown in Fig. 6. Such trigons became smaller and shallower with CVD treatment time, and finally disappeared when the triangular pits were filled up. These results suggest that trigons are formed not by being etched in the microwave plasma of CO–H_2 mixed gas, but by the joining of triangular growth layers under the present CVD conditions. Spreading layers joined as their steps touched each other and then formed larger growth layers. When growth layers with different thicknesses joined, the thicker layer was found to accommodate the thinner layer and continue to grow over it.

3.2. Topographical variation of {1 0 0} crystal surface

The growth process of the (1 0 0) crystal surface is shown in Fig. 7. The (1 0 0) surface pattern is composed of square growth layers piled up in the [1 0 0] direction to form a pyramidal growth hillock. Square growth layers spread in four [0 0 1] directions with treatment time. No screw pattern of the growth step was seen on lateral facets of the growth hillock [18]. Epitaxial two-dimensional nuclei tended to be formed at the same position. This was often the centre of the square growth layer, where supersaturation of the carbon source might be higher than in peripheral growing portions. Therefore, pyramidal steps would be formed by the repetition of two-dimensional nucleation at the same place and the subsequent progressive extension of the square layer.

When a two-dimensional nucleus ceased to generate, the hilltop of the pyramidal growth step changed into a terraced growth step with elapse of treatment time as shown in Fig. 7. When new epitaxial nuclei were formed at places other than the hilltop, a second pyramidal hillock began to be formed from the new nucleation point. The new hillock overlapped with the pyramidal hillock that had grown earlier. Fig. 8 shows the two overlapped pyramidal hillocks formed as a consequence of this process.

3.3. Discussion on the growth process of CVD diamond

It has been often pointed out that {1 1 1} surfaces of spontaneously nucleated CVD diamond crystals are rough, whereas {1 0 0} surfaces are smooth [7, 9]. Nevertheless the difference of growth mechanism of each crystal surface has not been clarified so far. The growth process observed in this work can give a reasonable explanation for such a different appearance between {1 1 1} and {1 0 0} surfaces. On {1 1 1} surfaces, a large number of epitaxial nuclei are formed at random, which may induce the surface roughness. On the other hand, epitaxial nuclei on {1 0 0} surfaces are formed repeatedly on the same position, which may result in the surface smoothness. The different appearance between {1 1 1} and {1 0 0} surfaces is attributed to the difference in growth mode.

As described above, epitaxial two-dimensional nuclei were formed more frequently on {1 1 1} surfaces, although a layer-by-layer growth process was observed on both {1 1 1} and {1 0 0} surfaces. More frequent nucleation on {1 1 1} surfaces can be explained by the fact that the {1 1 1} planes are close-packed planes. Carbon atoms which adsorbed from the vapour phase on to smooth {1 1 1} surfaces are bonded by the three nearest surface carbons, while those adsorbed on smooth {1 0 0} surfaces are bonded by the two nearest surface carbons. Therefore, carbon atoms which adsorbed on {1 1 1} surface are more strongly bound to given positions of the surface. They have a lower probability of desorption into the vapour phase and migration to the edge of growth layers than those adsorbed on {1 0 0} surface. Consequently, the {1 1 1} surface grows by a multiple nucleation mode,

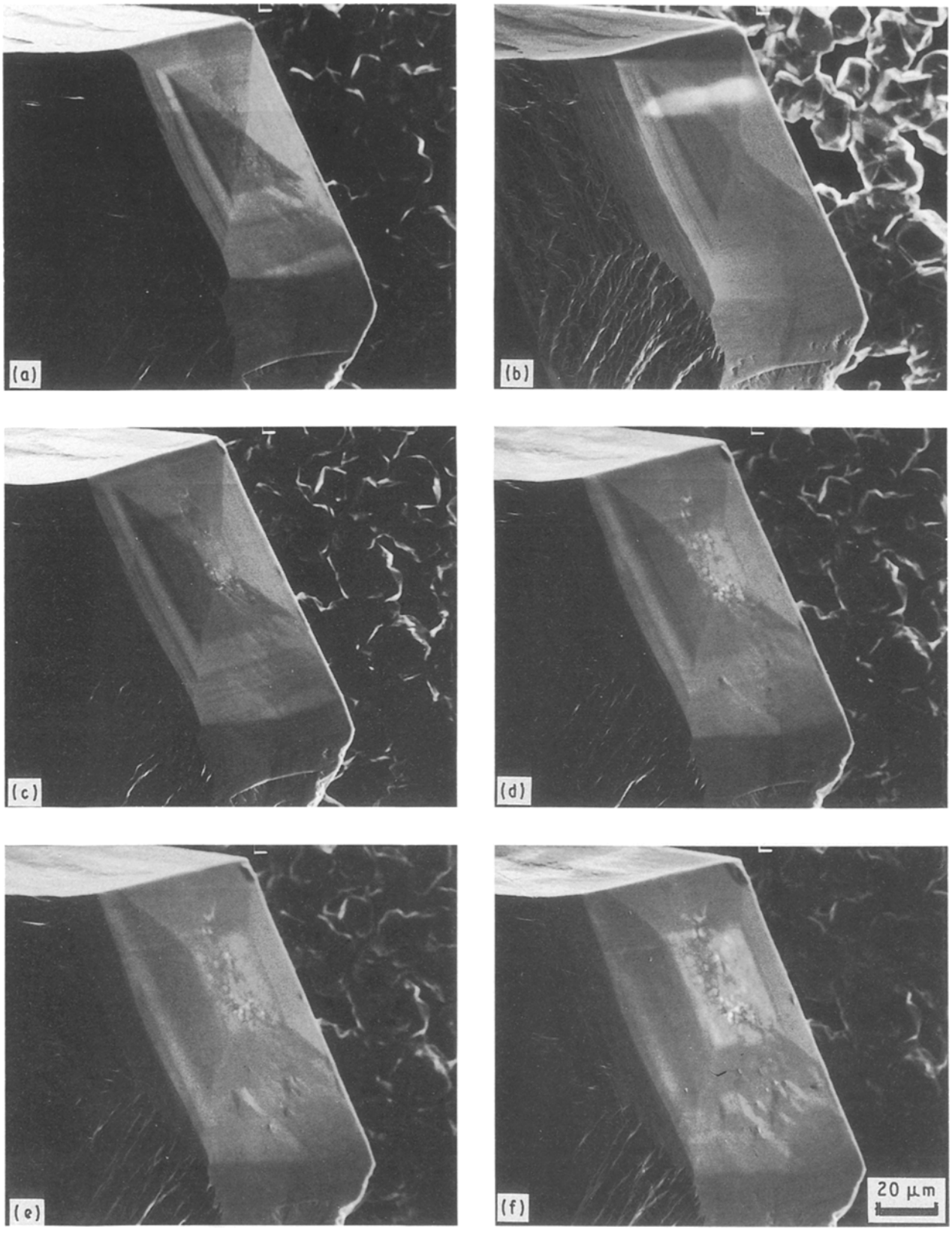

Figure 7 Topographical variation on (1 0 0) face of diamond single crystal with treatment time: (a) 20 h, (b) 22 h, (c) 24 h, (d) 26 h, (e) 28 h, (f) 30 h.

and the {1 0 0} surface grows by a single nucleation mode.

Microtopographs on {1 1 1} surfaces observed in our experiment are almost consistent with those of spontaneously nucleated diamond crystals [12–14]. A topography similar to the pyramidal growth hillock is also seen on {1 0 0} surfaces of diamond that spontaneously nucleated on a silicon substrate [16]. Therefore, it is considered that the growth process observed here can be applied to that of spontaneously nucleated diamond.

4. Conclusions

Surface topographical variations of diamond single crystals grown in the microwave plasma of the

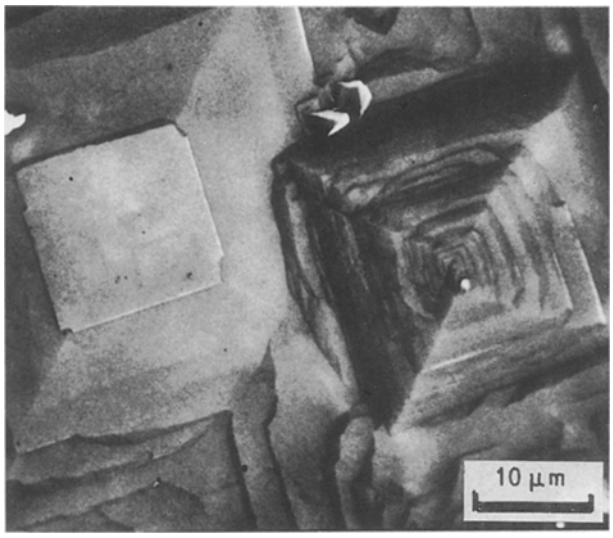

Figure 8 Two pyramidal growth hillocks overlapping each other.

CO–H_2 reactant gas system were observed by scanning electron microscopy. A layer-by-layer growth process was observed on both {1 1 1} and {1 0 0} crystal surfaces. The {1 1 1} planes are formed by multiple nucleation at random places and subsequent spreading of epitaxial triangular growth layers. When the triangular layers joined, a trigon which remained as an inverse triangular pit was observed. The {1 0 0} planes are formed by the repetition of two-dimensional nucleation at the same position and the spreading of square growth layers. These growth modes can be applied to interpret the roughness of {1 1 1} planes and the smoothness of {1 0 0} planes that are observed on spontaneously nucleated CVD diamond crystals. The dependence of the growth process on the growth conditions will be discussed in another paper [19].

References

1. B. V. SPITSYN, L. L. BOUILOV and B. V. DERJAGUIN, *J. Cryst. Growth* **52** (1981) 219.
2. M. KAMO, H. YURIMOTO and Y. SATO, *Appl. Surf. Sci.* **33/34** (1988) 553.
3. H. G. MAGUIRE, T. E. DERRY, W. S. BROOKS, J. P. F. SELLSHOP and M. KAMO, *South African J. Sci.* **84** (1989) 696.
4. C. F. CHEN, Y. C. MUANG and S. HOSOMI, *Hyomen Gijutu (J. Surface Finishing Soc. Jpn)* **40** (1989) 295.
5. H. SHIOMI, K. TANABE, Y. NISHIBAYASHI and N. FUJIMORI, *Jpn. J. Appl. Phys.* **29** (1990) 34.
6. D. G. JENG, H. S. TUAN, R. F. SALAT and G. J. FRICANO, *Appl. Phys. Lett.* **56** (1990) 1968.
7. S. MATSUMOTO, Y. SATO, M. TSUTSUMI and N. SETAKA, *J. Mater. Sci.* **17** (1982) 642.
8. M. KAMO, Y. SATO, S. MATSUMOTO and N. SETAKA, *J. Cryst. Growth* **62** (1983) 642.
9. J. S. KIM, M. H. KIM, S. S. PARK and J. Y. LEE, *J. Appl. Phys.* **63** (1990) 3354.
10. C. P. CHANG, D. L. FLAMM, D. E. IBBOTOSON and J. A. MUCHA, *ibid.* **63** (1988) 1744.
11. A. M. BONNOT, *Phys. Rev. B* **44** (1990) 6040.
12. K. HIRABAYASHI and N. I. KURIHARA, *Jpn. J. Appl. Phys.* **29** (1990) L1862.
13. *Idem., ibid.* **29** (1990) L1901.
14. *Idem., ibid.* **30** (1991) L 49.
15. H. ITOH, T. NAKAMURA, H. IWAHARA and H. SAKAMOTO, *J. Cryst. Growth* **108** (1991) 647.
16. H. ITOH, T. OSAKI, H. IWAHARA and H. SAKAMOTO, *J. Mater. Sci.* **26** (1991) 3763.
17. J. E. FIELD, "The Properties of Diamond" (Academic, London, 1979) pp. 245, 425.
18. H. ITOH, T. NAKAMURA, H. IWAHARA and H. SAKAMOTO, in Proceedings of 2nd International Conference on New Diamond Science and Technology, Washington DC, 1990, edited by R. Messier, J. J. Glass, J. E. Butter and R. Roy (Materials Research Society, Pittsburgh, 1991) pp. 479–484.
19. T. NAKAMURA, T. KAWAI, H. ITOH and H. IWAHARA, *J. Mater. Sci.* to be submitted.

Received 16 July 1991
and accepted 17 February 1992